

Communication

RAFT polymerization of N-[3-(trimethoxysilyl)propyl]acrylamide and its versatile use in silica hybrid materials

Anthony L. B. Maçon, Sarah L. Greasley, C. Remzi Becer* and Julian R. Jones*

Anthony L. B. Maçon, Sarah L. Greasley and Prof. Julian R. Jones
Department of Materials, Imperial College London, SW7 2AZ, London, UK.
E-mail: Julian.r.jones@imperial.ac.uk
Dr. C. Remzi Becer
School of Engineering and Materials Science, Queen Mary University of London, E1 4NS,
London, UK.
E-mail: r.becer@qmul.ac.uk

Abstract:

RAFT polymerization and characterization of an alkoxy silane acrylamide monomer using a trithiocarbonate chain transfer agent is described. Poly(*N*-[3-(trimethoxysilyl)propyl]acrylamide) (PTMSPAA) homopolymers were obtained with good control over the polymerization. A linear increase in the molecular weight was observed whereas the polydispersity values did not exceed 1.2 regardless of the monomer conversion. Moreover, PTMSPAA was used as a macro RAFT agent to polymerize *N*-isopropylacrylamide (NIPAM). By varying the degree of polymerization of NIPAM within the block copolymer, different sizes of thermoresponsive particles were obtained. These particles were stabilized by the condensation of the alkoxy silane moieties of the polymers. Furthermore, a co-network of silica and PTMSPAA was prepared using the sol-gel process. After drying, transparent mesoporous hybrids were obtained with a surface area of up to 400 m².g⁻¹.

1. Introduction

Alkoxy silyl-containing polymers (ACP) have been widely used for the preparation of hybrid materials because of their varied properties and high tailorability.[1] For instance, these polymers can interpenetrate and covalently bond to the growing silica network (Class II hybrid) during the sol-gel process, conferring unique properties due to the synergic nano-scale interaction of the inorganic and organic compounds.[2] ACPs can be synthesized either by functionalization of existing polymers with an organo-modified alkoxy silane precursors such as (3-glycidyoxypropyl)trimethoxysilane, where nucleophiles can attack the electrophilic carbon of the epoxide providing covalent coupling, or through the radical polymerization of monomers that contains silsesquioxane precursors.[3] The latter has gained considerable

interest due to the extensive development of living polymerization, in which polymers can be designed with fine control over their architecture, morphology and chemical structure.[4]

A variety of structures such as vesicles, spherical particles, nanowires or nano-plates have been synthesized through the self-organization of well defined block-copolymers incorporating 3-(alkoxysilyl)propyl methacrylate or acrylate as a stabilizing agent.[3c,5] However, these polymers are often made of monomers belonging to different classes, combining for instance acrylamide, methacrylate or styrene, adding a level of complexity to the polymerization as each class of monomer usually needs distinctive experimental conditions. This is particularly true with reversible addition-fragmentation chain-transfer (RAFT) polymerization where the rate of addition of the CTA to the propagating radical must be greater than the rate of propagation, which varies considerably depending of the monomer class.[6] In addition, the recent advances made in the synthesis of multiblock copolymers (up to 20 blocks) have opened new perspectives in designing a novel class of polymer, where alkoxy silane monomer could play a determinant role in stabilizing macro-structures. [7]

In this communication, we are describing for the first time the RAFT polymerization of *N*-[3-(trimethoxysilyl)propyl]acrylamide monomer and the use of the obtained homopolymers as a macro-RAFT agent in block copolymerization with NIPAM. Amphiphilic block copolymers were utilized in the formation of micelles through a self-assembly process whereas homopolymers were utilized in the hybrid formation through a sol-gel process. Detailed characterizations of polymers, nanoparticles and hybrid materials have been performed using a range of analytical techniques.

2. Experimental Section

Details about materials, instrumentation, and synthetic protocols are reported in the Supporting Information.

3. Results and Discussion

Table 1. Result of the RAFT polymerization of TMSPAA and its chain extension with NIPAM.

Run	Feed Ratio ^{a)}	Time ^{b)} (h)	Conv ^{c)} (%)	Actual Ratio ^{c)}	Mn ^{d)} (g.mol ⁻¹)	PDI ^{d)}
P1/homo	25	3	38	TMSPAA ₇	1330	1.07
P2/homo	25	6	54	TMSPAA ₁₄	2760	1.12
P3/homo	50	3	41	TMSPAA ₄₁	2680	1.12
P4/homo	50	5	56	TMSPAA ₂₈	4730	1.14
P5/homo	100	3	33	TMSPAA ₂₆	3720	1.11
P6/homo	100	6	45	TMSPAA ₄₅	5670	1.18
P7/homo	50	18	89	TMSPAA ₄₁	4500	1.27
P8/block	28/100	24	89	TMSPAA ₂₈ - <i>b</i> -NIPAM ₈₁	14310	1.18
P9/block	28/200	24	91	TMSPAA ₂₈ - <i>b</i> -NIPAM ₁₆₂	23460	1.19
P10/block	28/375	24	99	TMSPAA ₂₈ - <i>b</i> -NIPAM ₃₇₁	49400	1.10

a) Degree of polymerization targeted at 80% of conversion; b) Time at which an aliquot was taken or the reaction terminated by dipping the flask in liquid nitrogen; c) Determined by ¹H NMR; d) Determined by size exclusion chromatography calibrated with near-monodisperse pMMA calibrant in THF at 1 ml.min⁻¹.

N-[3-(trimethoxysilyl)propyl]acrylamide was polymerized by RAFT in THF at 60 °C using 2,2'-Azobisisobutyronitrile (AIBN) as an initiator. The results of the different polymerizations are summarized in Table 1. The monomer concentration was fixed at 1M as high cross-linking density polymers synthesized with alkoxy silane monomers have a tendency of condensing (forming Si-O-Si branching) at high conversions as the viscosity increases.[8] Trithiocarbonate chain transfer agent, butyl ether 2-(dodecylthiocarbonothioylthio)-2-methylpropionate, (CTA, ¹H NMR Figure S1) was selected for its high efficiency to polymerize the acrylamide class of monomer.[6,9] For all polymerizations, the molar ratio of initiator to CTA was held constant at 5:1 while the molar ratio monomer to CTA was varied, targeting polymer with theoretical molecular weight (calculated using $M_{n,Theo} = M_{w,CTA} + DP \times M_{w,monomer}$) of 6253 g.mol⁻¹ ([M]:[CTA]=25:1), 12085 g.mol⁻¹ ([M]:[CTA]=50:1) and

23750 g.mol⁻¹ ([M]:[CTA]=100:1), at 80% conversion. The monomer conversion was followed by ¹H NMR, taking aliquots of the polymerization solution at regular time intervals and comparing the relative integration of the closest protons to the silicon atom on the propyl chain to the vinyl protons of the monomer.

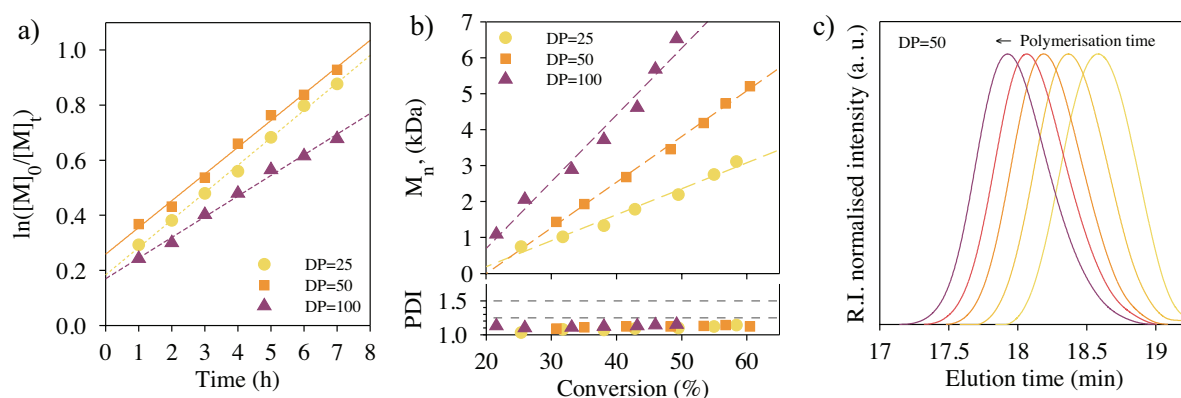


Figure 1. a) Pseudo first order kinetic plot for TTC-CTA mediated RAFT polymerization of N-[3-(trimethoxysilyl)propyl]acrylamide ($[M]_0 = 1 \text{ mol.L}^{-1}$ targeting a degree of polymerization of 25, 50 and 100 at 60 °C in THF. b) Average molecular weight of the growing polymer chains as a function of the monomer conversion determined by size exclusion chromatography using pMMA as calibrant and c) Elution graphs at different polymerization time points for DP = 50.

Figure 1-a shows that a linear pseudo-first order kinetics was obtained regardless of the molecular weight targeted, with 55% conversion reached at 6 hours of polymerization. Size exclusion chromatography (SEC) revealed that the number average molecular weight increased linearly as a function of conversion while the polydispersity indices (PDI) stayed below 1.2 (Figure 1-b & c).

Relatively low PDI values are a good indication of a controlled/living radical polymerization process. However, in order to demonstrate the high-chain end fidelity, obtained PTMSPAA homopolymers were used as a macro-RAFT agent for the copolymerization of *N*-isopropylacrylamide (NIPAM). Due to the instability of the alkoxy silane moiety upon purification and drying, the structural integrity of the polymer was measured by NMR.[3b]

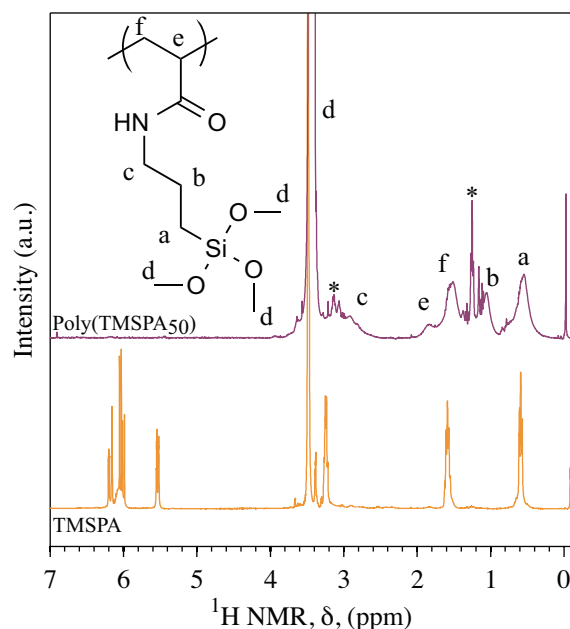


Figure 2. ^1H NMR spectra of *N*-[3-(trimethoxysilyl)propyl]acrylamide and its corresponding polymer with a degree of polymerization of 50 in CDCl_3 . * traces of THF.

Hence, ^1H NMR showed that with the experimental conditions used, no hydrolysis of the alkoxysilane moiety was triggered, with the integration of the methoxy protons ($\delta_{\text{SiOCH}_3} = 3.56$ ppm) being in good agreement with the monomer relative to the rest of the structure (Figure 2). Hydrolysis occurring during the purification would compromise the synthesis of block-copolymers with narrow molecular weight distribution, as possible condensation of the silanol could occur. Similar experimental conditions, as compared to TMSPAA, were used for the polymerization of NIPAM with a fixed monomer concentration of 1M and $[\text{M}]:[\text{TTC-CTA}]:[\text{I}]$ ratios of 100:1:0.2. The macro-RAFT used (**P3**) had a M_n of $2,700 \text{ g}\cdot\text{mol}^{-1}$ (PDI = 1.12) and the resulting block copolymer a calculated M_n of $14000 \text{ g}\cdot\text{mol}^{-1}$ with a narrow molecular weight distribution, PDI = 1.18 (^1H NMR, Figure S2). The SEC analysis of the block copolymer shows that when PTMSPAA was used as a macro-RAFT agent, high re-initiation efficiency was obtained with mono-modal distribution of the molecular weight (Figure S3). However, small humps on either side of the distribution could be observed. On the low molecular weight side, this could be attributed to dead macro-RAFT end-chain whereas it is likely that the high molecular weight shoulder originated from termination by

combination occurring towards the end of the polymerization when high monomer conversion was reached.

3.2. Versatile use of PTMSPAA as gelable polymer

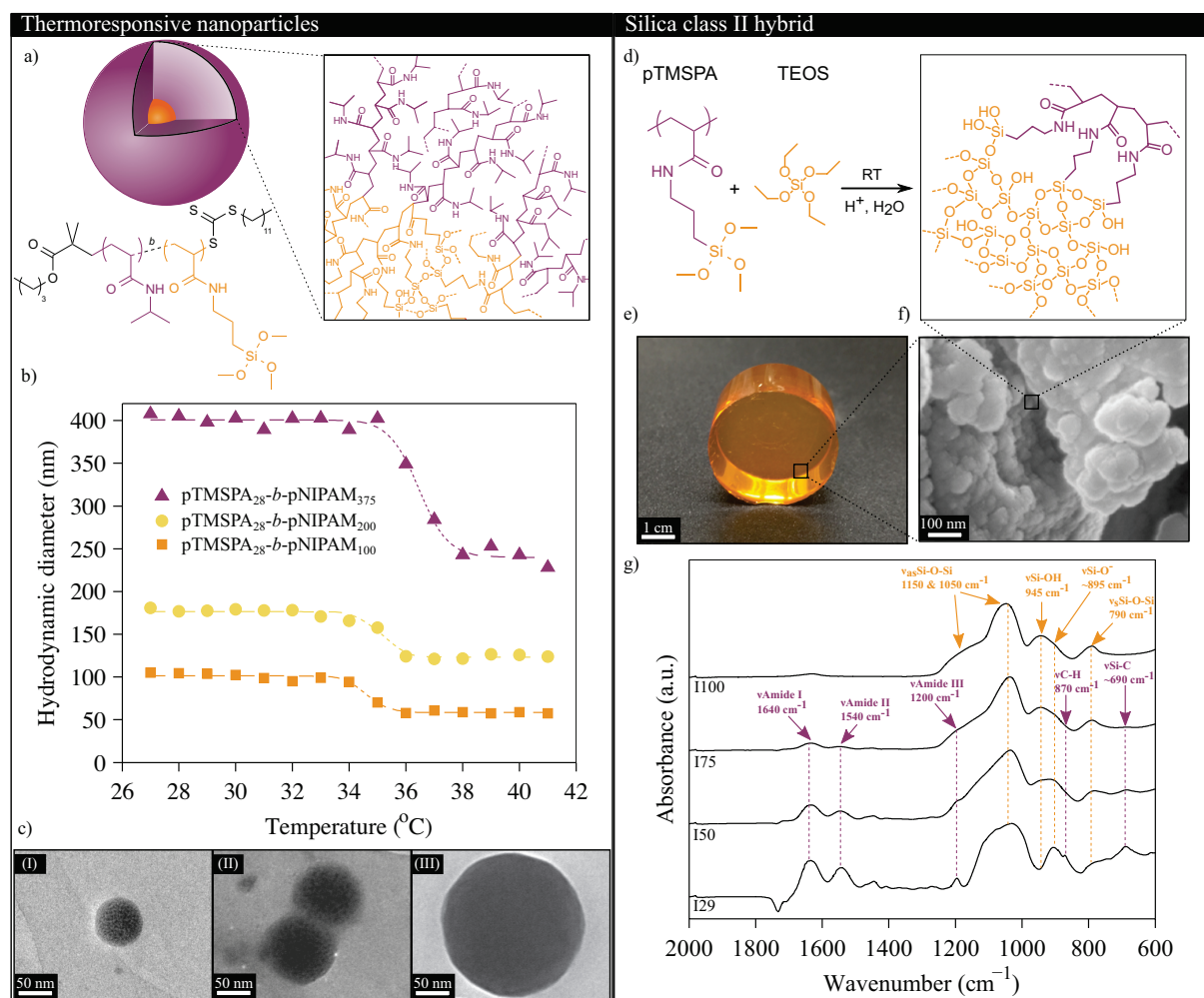


Figure 3. Demonstration of the versatile use of pTMSPAA: a) Structural representation of poly(TMSPAA-*b*-NIPAM) and a schematic representing the core-shell structure that was obtained by a precipitation method; b) Temperature response of the particle made with **P8**, **P9** and **P10** where the relative concentration of NIPAM to TMSPAA was varied and c) Corresponding TEM images; d) Schematic representing the synthesis of silica class II hybrid, using pTMSPAA as an organic source; e) and f) Conventional and SEM images of the resulting materials. g) ATR-FTIR of PTMSPAA/SiO₂ hybrid at different inorganic to organic ratios.

In this section, two examples of the versatile use of pTMSPAA are given with *i)* the synthesis of temperature responsive nanoparticles made from the block copolymer poly(TMSPAA-*b*-

NIPAM) (**P8**, **P9** and **P10**), and *ii*) the synthesis of silica class II hybrid using of pTMSPAA (**P7**) as a organic source and tetraethyl orthosilicate (TEOS) as an inorganic source *via* the sol-gel process.

3.2.1. Temperature responsive nanoparticles

Core-shell thermoresponsive nanoparticles made from poly(TMSPAA-*b*-NIPAM) were prepared using an adapted method proposed by Zhang *et al.* and shown in Figure 3-a.[5c] Briefly, the purified block copolymer was dissolved in dimethylformamide (DMF) at a concentration of 1 mM, in which both segments of the polymer were soluble. Then, a 5 mM triethylamine (TEA) solution was added drop-wise to DMF, which, above 15% v/v solvent ratio, induced self-assembly *via* micellation of the polymer, where the hydrophobic PTMSPAA formed the core of the particle and the NIPAM residues become the shell. The presence of TEA stabilized the particle by catalyzing the formation of Si-O-Si branching, through the condensation of the alkoxy silane moieties present in the core of the particles. Different sized particles could be synthesized by varying the degree of polymerization (DP) of the NIPAM segment during the chain extension, resulting in monomodal particles with narrow distribution of a hydrodynamic diameter ranging from 100 nm (**P8**, DP=100) to 400 nm (**P10**, DP=375), measured by dynamic light scattering (DLS) at 25 °C (Figure S4). Poly(NIPAM) is known to undergo a coil-to-globule transition when the temperature increases above its lower critical solution temperature (LCST), which is approximately 32 °C.[10] Thus, the temperature response of the particles was evaluated by DLS after dialysis of the particles against pH 7 water as shown in Figure 3-b. All the particles decreased in size above 32 °C, regardless of their original size. For instance, the hydrodynamic diameter of the particles made from poly(TMSPAA₂₅-*b*-NIPAM₂₀₀) decreased from 173.3±2.6 nm below 32 °C to 104.9±3.5 nm above 32 °C (Figure S5). The sizes of the particles after dehydration

(>32 °C) measured by DLS were in good agreement with the images taken in the vacuum environment of the transmission electron microscopy as shown in Figure 3-c (low magnification images are available in Figure S6).

3.2.2. Silica class II hybrid synthesis

Silicate class II hybrids, pTMSPAA/SiO₂, were synthesized *via* the sol-gel process by mixing hydrolyzed tetraethyl orthosilicate (TEOS) with pTMSPAA (**P4**) as shown in Figure 3-d. The relative concentration of pTMSPAA to TEOS was varied in order to control the inorganic to organic weight ratio (I_h), aiming at 29% (polymer only), 50%, 75% and 100% (control consisting of a pure silica gel). The addition of pTMSPAA had a significant effect on gelation time, decreasing as the I_h decreased, ranging from 3 days for $I_h = 100%$ to 2 minute for $I_h = 29%$ (Figure S7). After complete drying at 60 °C, optically transparent and crack free monoliths were obtained (Figure 3-e), regardless of the composition targeted. The morphology of PTMSPAA/SiO₂ hybrid revealed by SEM of its fractured surface showed aggregated colloidal particles, typical of silica sol-gel derived materials, often associated with a interstitial disordered mesoporous.[11] Thus, the specific surface area (SSA) of the pTMSPAA/SiO₂ hybrids was measured by nitrogen sorption, applying the BET method to the first eleven points of the adsorption branch (see full isotherms, Figure S8).[12] The SSA of the hybrid was found to be a function of the inorganic to organic ratio, decreasing from 457 m².g⁻¹ for I100 down to the detection limit of the instrument for I29 (see Figure S9). Thus, on the basis of the variation in gelation time and the SSA, the mechanism of gelation of these hybrids can be assumed to differ from these of pure tetraorthosilicate species. Variation in the molecular structure of hybrids as a function of I_h was monitored by attenuated total reflectance Fourier transform infrared (ATR-FTIR). Spectra were normalized to the asymmetric stretching band of Si-O-Si at 1050 cm⁻¹, present in all composition. At $I_h = 29%$,

the characteristic bands of the amide moiety were detected with C=O stretching at 1640 cm⁻¹ (amide I), N-H bending vibration at 1540 cm⁻¹ (amide II) and C-N vibration at 1200 cm⁻¹ (amide III), as well as infrared absorption band from the polymer backbone, C-H at 870 cm⁻¹. As the inorganic to organic weight ratio increased, the intensity of the absorption bands of the pTMSPAA decreased relative to the silica network (Si-O-Si).

4. Conclusions

In this report, *N*-[3-(trimethoxysilyl)propyl]acrylamide was successfully polymerized, in a controlled manner (PDI < 1.2), by RAFT using a trithiocarbonate chain transfer agent without triggering any hydrolysis of the alkoxy silane moiety. After purification, PTMSPAA showed a high efficiency to reinitiate chain growth, confirming the living nature of the polymerization. PTMSPAA was proven to be very versatile in its use as a gelable polymer through the formation of thermoresponsive nanoparticle with size ranging from 100 to 400 nm, depending on the degree of polymerization of the NIPAM residue and silica class II hybrid at different inorganic to organic ratios. The data acquired herein shows that TMSPAA could potentially to be used as a structural agent for advance sequential polymerization.

Supporting Information

Supporting Information is available from the Wiley Online Library or from the author.

Acknowledgements: The authors wish to thank EPSRC (EP/I020861/1) for funding.

Received: Month XX, XXXX; Revised: Month XX, XXXX; Published online:

((For PPP, use “Accepted: Month XX, XXXX” instead of “Published online”)); DOI:

10.1002/marc.((insert number)) ((or ppap., mabi., macp., mame., mren., mats.))

Keywords: *N*-[3-(trimethoxysilyl)propyl]acrylamide, RAFT, NIPAM, Thermoresponsive nanoparticles, Sol-gel class II hybrid.

References:

[1] a) M. Beija, J-D. Marty, and M. Destarac. *Prog. Polym. Sci.* **2011**, *36*, 845–886. b) Y. Chen, J. Du, M. Xiong, and H. Zhu. *Macromol. Rapid Commun.* **2006**, *27*, 741–750. c) C. Sanchez, C. Boissiere, S. Cassaignon, C. Chaneac, O. Durupthy, M. Faustini, D. Grosso, C. Laberty-Robert, L. Nicole, D. Portehault, F. Ribot, L. Rozes, and C. Sassoie. *Chem. Mater.* **2014**, *26*, 221–238.

[2] a) B. M. Novak. *Adv. Mater.* **1993**, *5*, 422–432. b) O. Mahony, O. Tsigkou, C. Ionescu, C. Minelli, L. Ling, R. Hanly, M. E. Smith, M. M. Stevens, and J. R. Jones. *Adv. Funct. Mater.* **2010**, *20*, 3835–3845.

[3] a) L. S. Connell, F. Romer, M. Suárez, E. M. Valliant, Z. Zhang, P. D. Lee, M. E. Smith, J. V. Hanna, and J. R. Jones. *J. Mater. Chem. B.* **2014**, *2*, 668. b) V. Mellon, D. Rinaldi, E. Bourgeat-Lami, and F. D’agosto. *Macromolecules.* **2005**, *38*, 1591–1598. c) J. Du and Y. Chen. *Macromolecules.* **2004**, *37*, 6322–6328.

[4] a) A. Gregory and M. H. Stenzel. *Prog. Polym. Sci.* **2012**, *37*, 38–105. b) K. Kempe, A. Krieg, C. R. Becer, U. S. Schubert. *Chem. Soc. Rev.* **2012**, *41*, 176–191.

[5] a) K. Zhang, L. Gao, C. Zhang, and Y. Chen. *J. Mater. Chem.* **2009**, *19*, 3482–3489. b) K. Zhang, L. Gao, and Y. Chen. *Macromolecules.* **2007**, *40*, 5916–5922. c) Y. Zhang, S. Luo, and S. Liu. *Macromolecules*, **2005**, *38*, 9813–9820. d) J. Yuan, Y. Xu, A. Walther, S. Bolisetty, M. Schumacher, H. Schmalz, M. Ballauff, and A. H. E. Muller. *Nat. Mat.* **2008**, *7*, 718–722. e) M. Xiong, Y. Chen, and M. Maskos. *Macromol. Rapid Commun.* **2008**, *29*, 1368–1371. f) B. Peng, Y. Liu, Z. Li, and Y. Chen. *Soft Matter.* **2012**, *8*, 12002–12008. g) M. Mullner, J. Yuan, S. Weiss, A. Walther, M. Fortsch, M. Drechsler, and A. H. E. Muller. *J.*

- Am. Chem. Soc.* **2010**, *132*, 16587–16592. h) W. Li, C-H. Kuo, I. Kanyo, S. Thanneeru, and J. He. *Macromolecules*. **2014**, *47*, 5932–5941. i) C. G. Gamys, E. Beyou, and E. Bourgeat-Lami. *J. Polym. Sci. Pol. Chem.* **2010**, *48*, 784–793. j) H. Wei, C. Cheng, W-Q. Chen, S-X Cheng, X-Z. Zhang and R-X. Zhuo, *Langmuir*. **2008**, *24*, 4564-4570.
- [6] D. J. Keddie, G. Moad, E. Rizzardo, and S. H. Thang. *Macromolecules*. **2012**, *45*, 5321–5342.
- [7] a) G. Gody, T. Maschmeyer, P. B. Zetterlund, and S. Perrier. *Nat. Commun.* **2013**, *4*, 2505. b) L. Martin, G. Gody, and S. Perrier. *Polym. Chem.* **2015**. DOI: 10.1039/C5PY00478K
- [8] M. Xiong, K. Zhang, and Y. Chen. *Eur. Polym. J.* **2008**, *44*, 3835–3841.
- [9] A. J. Convertine, N. Ayres, C. W. Scales, A. B. Lowe, and C. L. McCormick. *Biomacromolecules*. **2004**, *5*, 1177–1180.
- [10] H. G. Schild. *Prog. Polym. Sci.* **1992**, *17*, 163–249.
- [11] C. J. Brinker and G. W. Scherer. *Sol-Gel Science: The Physics and Chemistry of Sol-Gel Processing*. Academic Press, San Diego, **1990**.
- [12] S. Brunauer, P. H. Emmett, and E. Teller. *J. Am. Chem. Soc.* **1938**, *60*, 309–319.

Table of contents:

The RAFT polymerization of poly(N-[3-(trimethoxysilyl)propyl]acrylamide) (PTMSPAA) is reported for the first time. Kinetic study and structural characterization of the polymer is shown. PTMSPAA is chain extended with NIPAM and used for the preparation of thermoresponsive nanoparticles. PTMSPAA can be used as an organic precursor for the synthesis of sol-gel class II hybrid.

